Electronic Supplementary Material (ESI) for Journal of Materials Chemistry A.
This journal is © The Royal Society of Chemistry 2022

# Wood-derived Flexible Supercapacitors for Anti-Freezing Green Power Sources

Hongting Ma,[a] Qian Zhao,[a] Peihao Cheng,[a] Xiaodong Geng,[a] Huannuo Tao,[a] Zhouxiaolong Zhang,[a] Yue Jiang,[a] Junlin Ma,[a] Kai Yang,[a] Quanli Liu,[a] Hanwen Zhang,[a] Zhida Liang,[b] Jian Li*[,c], Tianlu Wang,*[,a,d,e] Mianqi Xue,*[,f] and Nan Zhu*[,a]

[a] Cancer Hospital of Dalian University of Technology, School of Chemistry, Dalian University of Technology, Dalian, Liaoning, 116024, China.

[b] Department of Health Management, Dalian Rehabilitation Recuperation Center of Joint Logistics Support Force of PLA, Dalian,116013, China

[c] Center for Reproductive Medicine, Dalian Women and Children's Medical Center (Group), Dalian, 116037, China

[d] Department of Radiotherapy, Cancer Hospital of China Medical University, Liaoning, Cancer Hospital & Institute, Cancer Hospital of Dalian University of Technology, No.44, Xiaoheyan Road, Dadong District, Shenyang, 110042, Liaoning Province, China.

[e] Faculty of Medicine, Dalian University of Technology, Dalian 116024, China

[f] Technical Institute of Physics and Chemistry, Chinese Academy of Sciences, Beijing 100190, China.

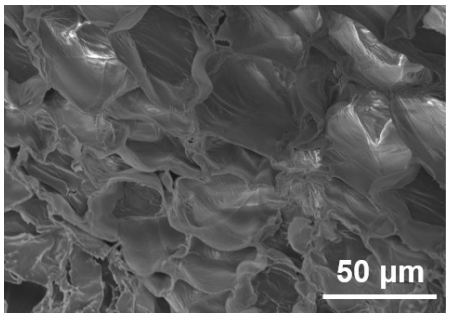


**Fig. S1.** SEM image of natural balsa wood.

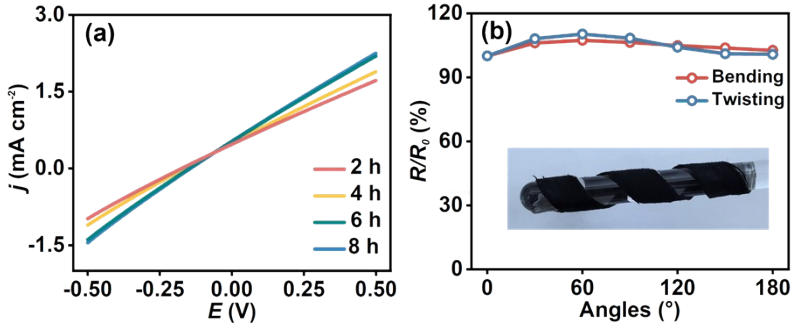


**Fig. S2.** (a) IV curves of PPy/ADW immersing in pyrone for 2, 4, 6, and 8 h. (b) Relative resistance change of PPy/ADW under different bending/twisting angles.

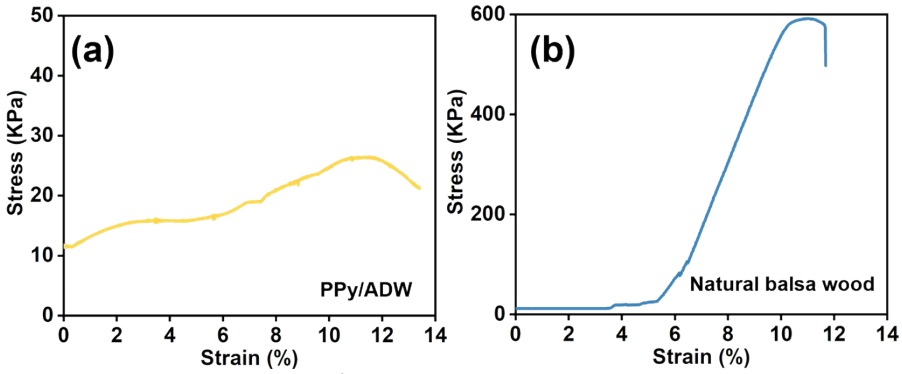


**Fig. S3.** Stress-strain curves of (a) PPy/ADW electrode, and (b) natural balsa wood under bending.

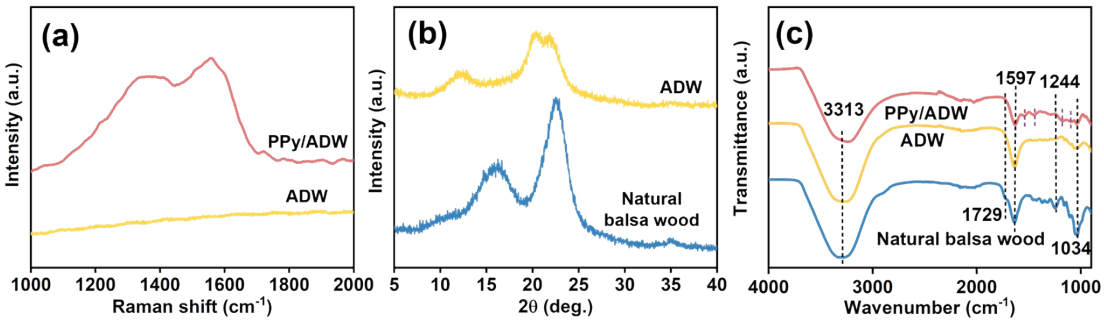


**Fig. S4.** (a) Raman, (b) XRD, and (c) FTIR spectra of natural balsa wood, ADW and PPy/ADW electrode..

As shown in Fig. S4a, the Raman spectrum of PPy/ADW electrode showed the C=C backbone stretching at ~1563 $cm^{-1}$ and the ring stretching mode of PPy at 1356 $cm^{-1}$, which were not observed in ADW.[1] The appearance of these two peaks indicated the successful polymerization of pyrrole on ADW.

Meanwhile, the physicochemical performance of natural balsa wood, and ADW samples were further studied by XRD. As shown in Fig. S4b, the typical signatures of a cellulose I structure with two broad crystalline reflections were observed in natural balsa wood at 16.3° and 22.6°, which were indexed as (101) and (002), respectively.[2] After delignification and alkali treatment, new peaks at 12.3° and 20° appeared in ADW, indicating mercerization and conversation of native cellulose (cellulose I) into another crystal form (cellulose II).[3]

Moreover, the hydroxyl groups of cellulose and C-O stretching of the cellulose structure contributing to the absorption bands at 3313 $cm^{-1}$ and 1034 $cm^{-1}$, respectively, were observed in natural balsa wood (Fig. S4c).[4] The characteristic lignin peaks at 1729 $cm^{-1}$ (C=O stretching in unconjugated ketone, carbonyl and aliphatic groups (xylan); C=O vibration of esters, ketones and aldehydes in hemicelluloses), 1597 $cm^{-1}$ (aromatic skeletal vibrations) and 1244 $cm^{-1}$ (C−O stretching vibration of acyl groups in lignin and hemicellulose) tended to be weaker or even disappeared in ADW, indicating significant removal of lignin and hemicellulose.[5, 6] In addition, the bands at 1034 $cm^{-1}$ for ADW were weaker than for the untreated sample because of the decreased cellulose crystallinity.[4] These changes confirmed the removal of hemicellulose and lignin in ADW sample. Characteristic peaks at 1541 and 1449 $cm^{-1}$ (pyrrole ring vibration), 1175 $cm^{-1}$ (C-C ring stretching) and 1093 $cm^{-1}$ (C-H in-plane vibrations) were observed in PPy/ADW, confirming that PPy was successfully grown into ADW.[7]

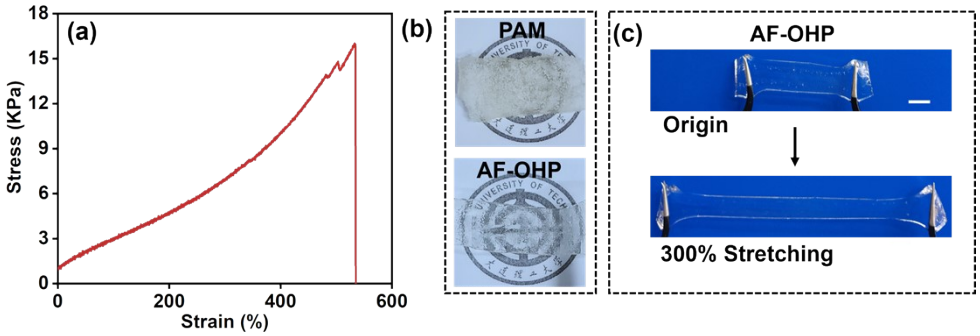


**Fig. S5.** (a) Stress-strain curves of AF-OHP hydrogel under stretching. (b) Photographs of PAM and AF-OHP at -30 °C. (c) Stretchability of AF-OHP before or under 300% tensile strains, with the scale bar of 1 cm.

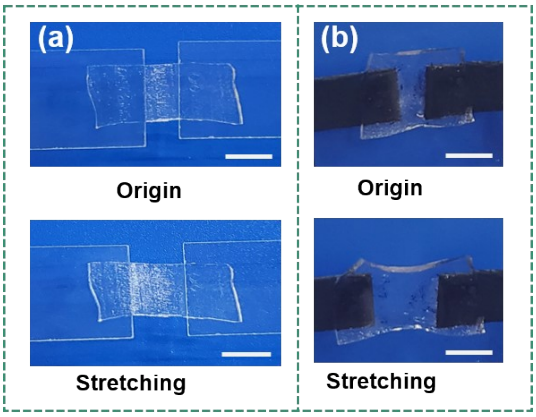


**Fig. S6**. AF-OHP stably adhered to (a) glass, (b) PPy/ADW without extra adhesives, with the scale bar of 1 cm.

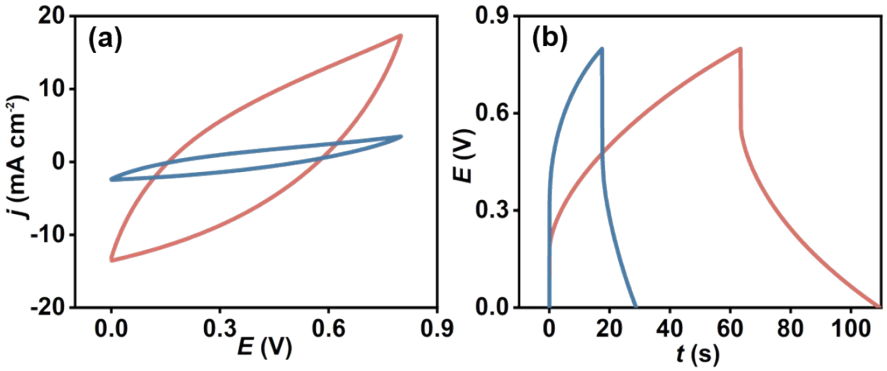


**Fig. S7**. (a) CV (100 mV $s^{-1}$) and (b) GCD curves (6 mA $cm^{-2}$) of natural balsa wood-based SC (blue line) and AF-FSC (red line).

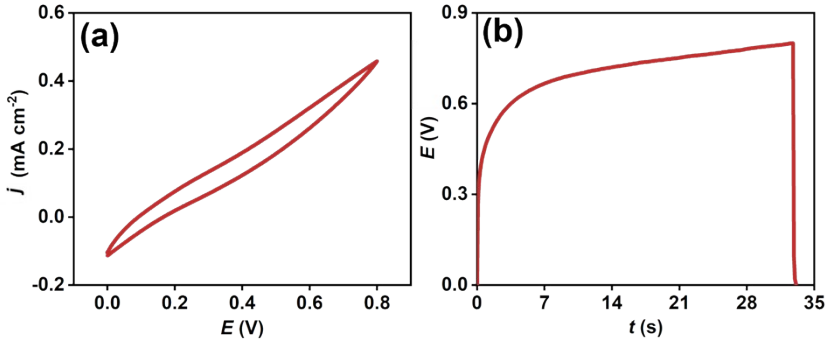


**Fig. S8**. (a) CV (100 mV $s^{-1}$) and (b) GCD curves (0.2 mA $cm^{-2}$) of PET-based SC.

The PPy coated polyethylene terephthalate (PET) electrode (PPy/PET) was prepared through chemical oxidative polymerization process. The PET substrate was first etched by oxygen plasma at 180 W for 5 min to become hydrophilic. Then treated PET substrate was immersed in 0.6 M pyrrole solution with dissolved (Ammonium persulfate) APS (pyrrole/APS molar ratio =1:2) at 4°C for 6 hours. After completely polymerization of pyrrole, the electrode was taken out and washed with deionized water.

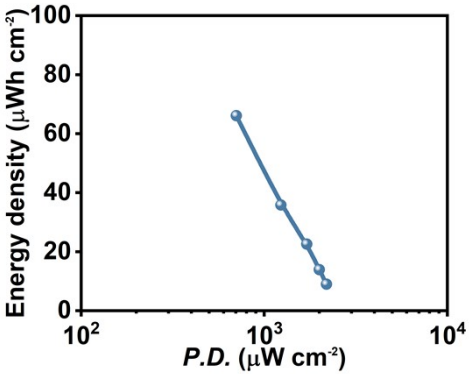


**Fig. S9.** Ragone plots of the AF-FSC.

**Table S1.** Volume-specific capacitance, energy density, and power density of AF-FSC

| Current density ($mA\ cm^{-2}$) | Volume capacitance ($mF\ cm^{-3}$) | Energy density ($\mu Wh\ cm^{-3}$) | Power density ($\mu W\ cm^{-3}$) |
|---|---|---|---|
| 2 | 10349.4 | 661.3 | 7083.9 |
| 4 | 6794.3 | 358.3 | 12323.2 |
| 6 | 5049.4 | 226.1 | 17064.2 |
| 8 | 4044.9 | 139.5 | 19942.8 |
| 10 | 3382.9 | 89.9 | 21867.6 |

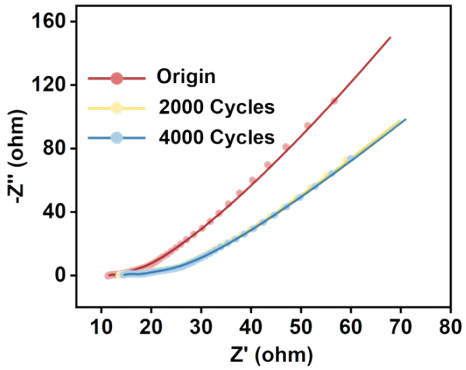


**Fig. S10**. Nyquist plot of the AF-FSC after 0, 2000 and 4000 testing cycles.

**Table S2**. Fitted EIS data for AF-FSC after 0, 2000, and 4000 testing cycles from Z-view software..

| Testing cycles | Rs (Ω) | Rct (Ω) |
|---|---|---|
| 0 | 11.35 | 2.007 |
| 2000 | 13.31 | 2.488 |
| 4000 | 14.06 | 2.644 |

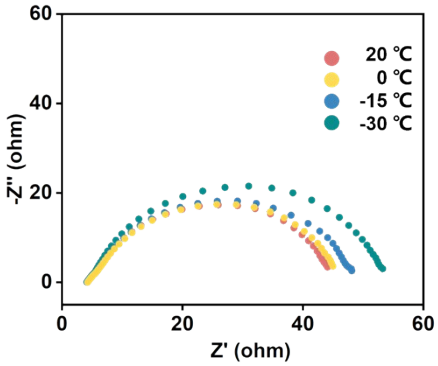


**Fig. S11.** AC impedance spectra of the AF-OHP electrolytes at 20, 0, -15, and -30 °C.

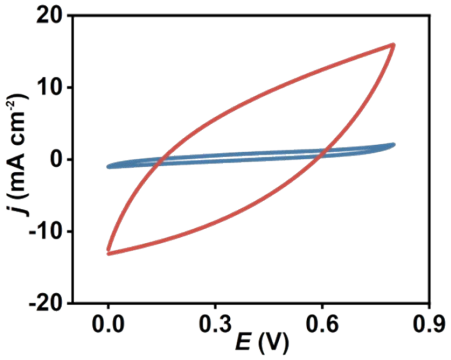


**Fig. S12**. CV curves (100 mV $s^{-1}$) of PAM-based SC (blue line) and AF-FSC (red line) at -30 °C.

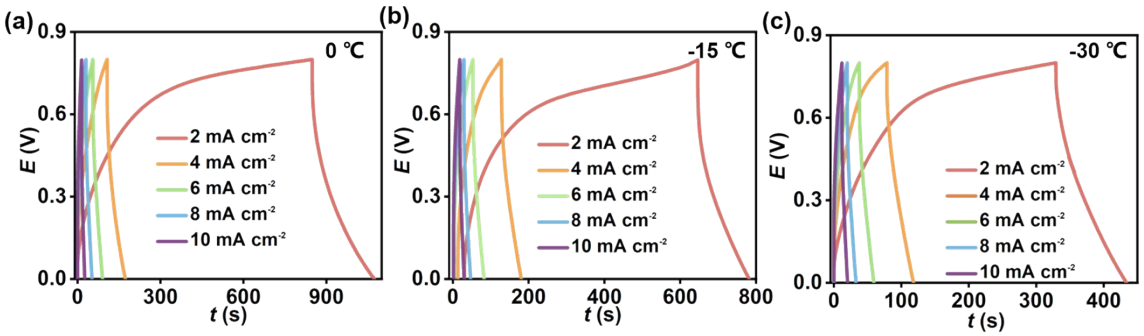


**Fig. S13.** GCD curves of AF-FSC at 0, -15, -30 °C.

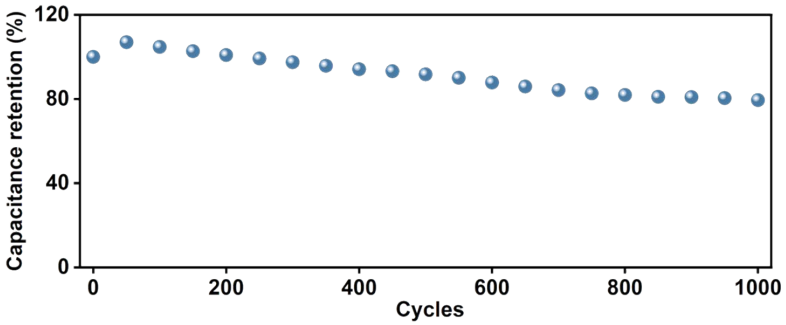


**Fig. S14.** Capacitance retention of AF-FSC during 1000 cycles at -30 °C. Scan rate of 100 mV $s^{-1}$.

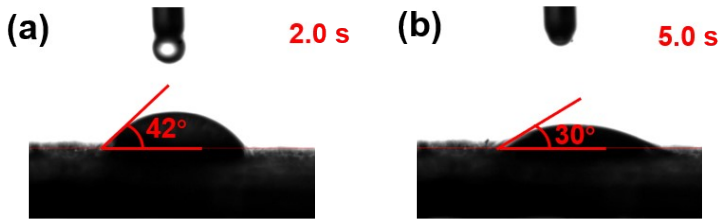


**Fig. S15.** Contact angle of PPy/natural balsa wood after dropping a water droplet for (a) 2.0 s, (b) 5.0 s at 20 °C.

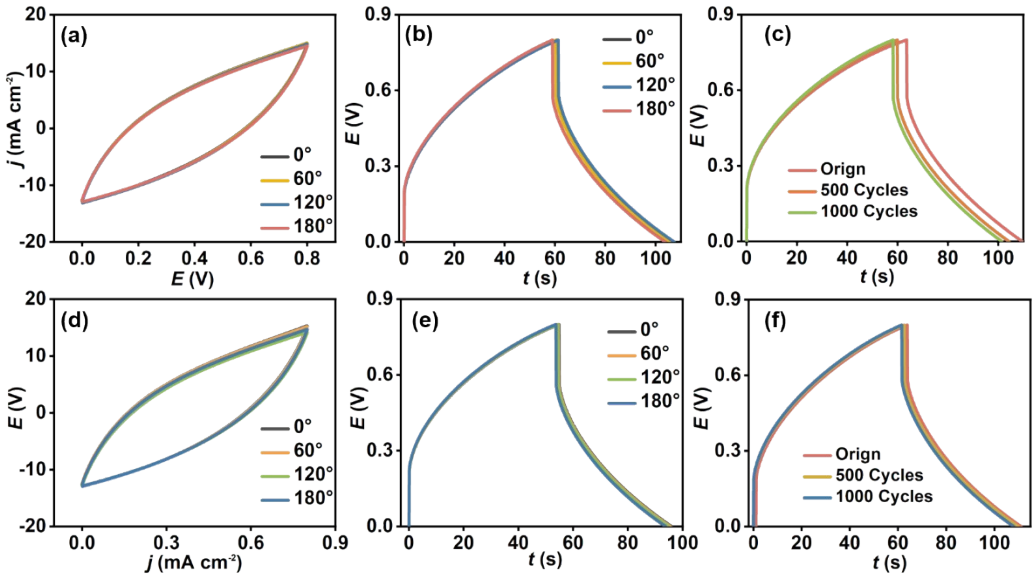


**Fig. S16.** Bending, stretching and cycling of AF-FSC at 20 °C. Electrochemical performance of AF-FSC under different bending ratios (a) CV curves (100 mV $s^{-1}$) and (b) GCD curves (6 mA $cm^{-2}$). (c) GCD curves (6 mA $cm^{-2}$) of 0, 500 and 1000 cycles bending-releasing cycles. Electrochemical performance of AF-FSC under different bending angles (d) CV curves (100 mV $s^{-1}$) and (e) GCD curves (6 mA $cm^{-2}$). (f) GCD curves (6 mA $cm^{-2}$) of 0, 500 and 1000 cycles bending-releasing cycles.

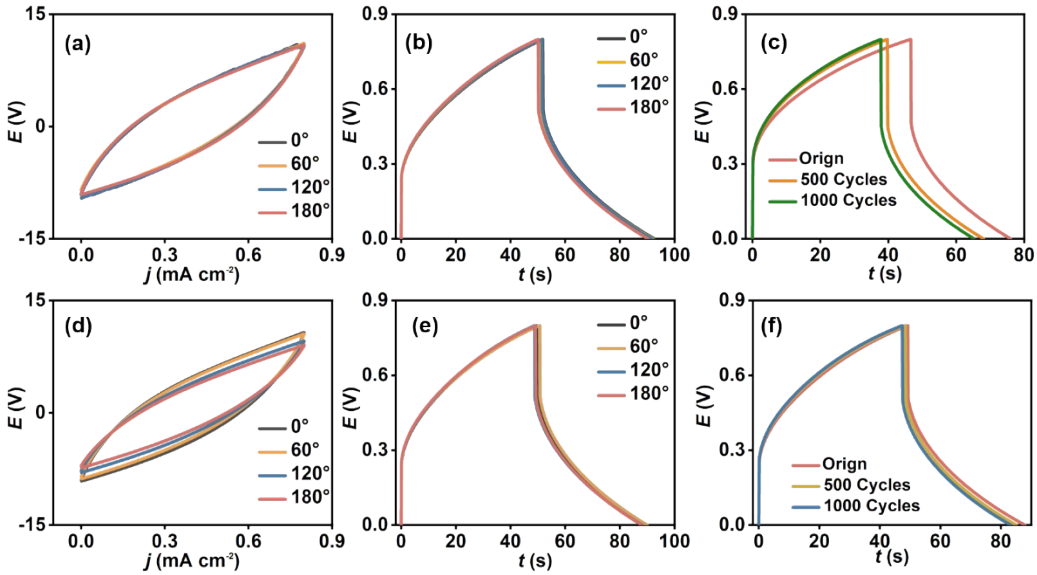


**Fig. S17.** Bending, stretching and cycling of AF-FSC at -30 °C**.** Electrochemical performance of AF-FSC under different bending ratios (a) CV curves (100 mV $s^{-1}$) and (b) GCD curves (4 mA $cm^{-2}$). (c) GCD curves (4 mA $cm^{-2}$) of 0, 500 and 1000 cycles twisting-releasing cycles. Electrochemical performance of AF-FSC under different twisting angles (d) CV curves (100 mV $s^{-1}$) and (e) GCD curves (4 mA $cm^{-2}$). (f) GCD curves (4 mA $cm^{-2}$) of 0, 500 and 1000 cycles twisting-releasing cycles.

## References

1. J. W. Park, S. J. Park, O. S. Kwon, C. Lee, J. Jang, *Analytical Chemistry,* 2014, **86** (3), 1822-1828.
2. C. Chen, Y. Wang, Q. Wu, Z. Wan, D. Li, Y. ; Jin, *Chemical Engineering Journal,* 2020, **400**, 125876.
3. K. Abe, H. Yano, *Carbohydrate Polymers*, 2011, **85** (4), 733-737.
4. N. Li, W. Chen, G. Chen, and J. Tian, *Carbohydr Polym*, 2017, **171**, 77-84.
5. X. Yang, F. Berthold, and L. A., *Biomacromolecules*, 2018, **19**, 3020-3029.
6. J. Song, C. Chen, C. Wang, Y. Kuang, Y. Li, F. Jiang, Y. Li, E. Hitz, Y. Zhang, B. Liu, A. Gong, H. Bian, J. Y. Zhu, J. Zhang, J. Li, and Hu, *ACS Appl Mater Interfaces*, 2017, **9**(28), 23520-23527.
7. Y. Chai, H. Ma, X. Ma, X. Zhang, Y. He, Y. Wang, Q. Jiang, X. Wang, J. Ji, and M. Xue, *Journal of Materials Chemistry A*, 2020, **8**, 10891-10897.